



KCC-1 Supported Ruthenium-Salen-Bridged Ionic Networks as a Reusable Catalyst for the Cycloaddition of Propargylic Amines and CO₂

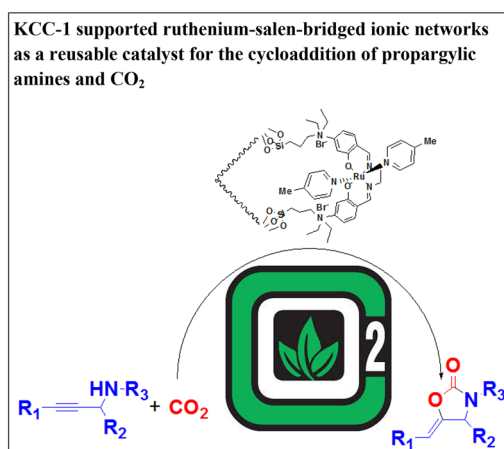
Seyed Mahdi Saadati¹ · Seyed Mohsen Sadeghzadeh²

Received: 27 December 2017 / Accepted: 24 February 2018
© Springer Science+Business Media, LLC, part of Springer Nature 2018

Abstract

This study investigates the potential application of an efficient, easily recoverable and reusable KCC-1 nanoparticle-supported Salen/Ru(II) catalyst in the synthesis of 2-oxazolidinones from CO₂, and propargylic amines. The KCC-1/Salen/Ru(II) NPs were thoroughly characterized by using TEM, SEM, TGA, FT-IR, ICP-MS, and BET. This observation was exploited in the direct and selective chemical fixation of CO₂, affording high degrees of CO₂ capture and conversion. The recycled catalyst has been analyzed by ICP-MS showing only minor changes in the morphology after the reaction, thus confirming the robustness of the catalyst.

Graphical Abstract



Keywords Nano catalyst · KCC-1 · One-pot synthesis · Green chemistry · CO₂

1 Introduction

Morphology-controlled nanomaterials such as silica play a decisive role in the development of technologies for addressing challenges in the fields of wellness, environment, and energy. Mesoporous silica materials discovery such as MCM-41 and SBA-15, a notable increase in the design. The synthesis of nano silica with different sizes, shapes, morphologies, and tissue properties have been observed in late years. KCC-1 is dendritic fibrous nanosilica as one notable

✉ Seyed Mahdi Saadati
smsaadati@bojnourdiau.ac.ir

¹ Department of Chemistry, Bojnourd Branch, Islamic Azad University, Bojnourd, Iran

² Young Researchers and Elite Club, Neyshabur Branch, Islamic Azad university, Neyshabur, Iran

invention that have a unique fibrous morphology, unlike the tubular porous structure of various customary silica materials. It has a high surface area with improved accessibility to the internal surface, tunable pore size and pore volume, controllable particle size, and, importantly, improved stability [1–10].

Carbon dioxide as a recyclable, non-toxic, easily available, naturally abundant, non-flammable and inexpensive C1 resource and considered as one of the most substantial greenhouse gases which caused the global warming and climate change [11–16]. As a result, the efficient change of carbon dioxide into useful chemicals is an important contribution from the opinion of environmental conservation and exploitation of resources [17–20]. The reaction of CO₂ with other organic compound to form the multi-membered cyclic carbonates has been extensively studied [21]. One of the useful methods for chemical fixation of CO₂ is the carboxylative cyclization of propargylic amines with CO₂ to provide 2-oxazolidinones [22–26]. Various investigations have been conducted for this reaction catalyzed by organometallic complexes of noble metals such as ruthenium [27], palladium [28], silver [29], and gold [30]. Organometallic complexes can reduce the cost and avoid the pollution caused by metals have been used for the carboxylative cyclization of propargylic amines with CO₂.

Ruthenium complexes are at the moment investigated because of their interesting structural, electrochemical, catalytic, and biological attributes [31–36] including research of ruthenium complexes containing diimino tetradentate Schiff bases, such as salen and salophen ligands [37, 38]. Recently, a number of ruthenium-salen complexes have also been found to be active catalysts in various chemical transformations [39, 40]. Specifically, ruthenium macrocyclic complexes which are stable to the side demetalation have been found to show a reversible electrochemistry and provide good model systems for mechanistic researches of proton-coupled multielectron transfer reactions [41, 42]. To

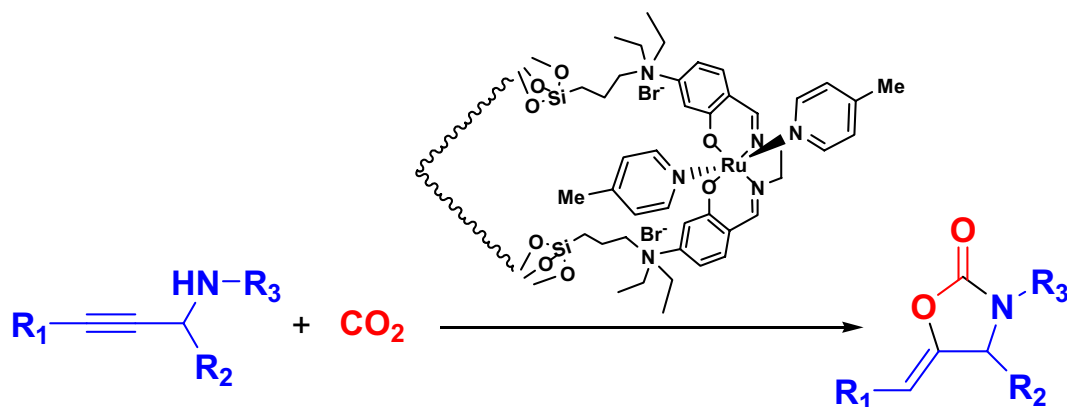
plan logically transformations catalyzed by ruthenium-salen complexes, the science of their redox and structural attributes is desirable [43].

Lately, organometallic ionic complexes (OICs) have emerged as very marvelous catalysts because they can be created from readily available and highly tailorable metal and ligand forerunners for multifunctional integration [44, 45]. Many researchers have shown OICs that contain a Lewis acidic metal center and a nucleophilic halogen anion (X[−]) portion as highly impressive bifunctional catalysts for the coupling reaction between carbon dioxide and other organic compound under co-catalyst free circumstances owing to the cooperative effects of the catalytic functional groups [46–48]. Having this point in mind, we envisioned a way in which the preface of Lewis acid (metal center) active sites to a halogen anion (X[−]) based ionic polymer could provide highly active, recyclable catalysts for the synthesis of cyclic carbonates. Herein, we report the design and synthesis of a novel bifunctional complex composed of the cross-linked KCC-1 as a substrate with the *N,N'*-bis{(4-dimethylamino)salicylidene}ethylenediamino ruthenium(II) [Salen-Ru(II)] Schiff base outer shell to serve as a catalyst for the synthesis 2-oxazolidinones from CO₂, and propargylic amines under solvent-free (Scheme 1).

2 Experimental

2.1 Materials and Methods

Chemical materials were purchased from Fluka and Merck in high purity. Melting points were determined in open capillaries using an Electrothermal 9100 apparatus and are uncorrected. FTIR spectra were recorded on a VERTEX 70 spectrometer (Bruker) in the transmission mode in spectroscopic grade KBr pellets for all the powders. The particle size and structure of nano particle was observed by using



Scheme 1 Synthesis of 2-oxazolidinones in the presence of KCC-1/Salen/Ru(II) NPs

a Philips CM10 transmission electron microscope operating at 100 kV. Powder X-ray diffraction data were obtained using Bruker D8 Advance model with Cu $\text{K}\alpha$ radiation. The thermogravimetric analysis (TGA) was carried out on a NETZSCH STA449F3 at a heating rate of $10\text{ }^{\circ}\text{C min}^{-1}$ under nitrogen. ^1H and ^{13}C NMR spectra were recorded on a BRUKER DRX-300 AVANCE spectrometer at 300.13 and 75.46 MHz, BRUKER DRX-400 AVANCE spectrometer at 400.22 and 100.63 MHz, respectively. Elemental analyses for C, H, and N were performed using a Heraeus CHN-O-rapid analyzer. The purity determination of the products and reaction monitoring were accomplished by TLC on silica gel polygram SILG/UV 254 plates. Mass spectra were recorded on Shimadzu GCMS-QP5050 mass spectrometer.

2.2 General Procedure for the Preparation of KCC-1 NPs

Tetraethyl orthosilicate (TEOS) (2.5 g) was dissolved in a solution of cyclohexane (30 mL) and 1-pentanol (1.5 mL). A stirred solution of cetylpyridinium bromide (CPB 1 g) and urea (0.6 g) in water (30 mL) was then added. The resulting mixture was continually stirred for 45 min at room temperature and then placed in a Teflon-sealed hydrothermal reactor and heated $120\text{ }^{\circ}\text{C}$ for 5 h. The silica formed was isolated by centrifugation then washed with a mixture of deionized water and acetone, and dried in a drying oven. This material was then calcined at $550\text{ }^{\circ}\text{C}$ for 5 h in air.

2.3 General Procedure for the Preparation of Salen

The salen ligand was prepared by modification of a previously reported procedure [49]. Diethylamine (0.30 g) was added to a solution of 4-(diethylamino)salicylaldehyde (2.00 g) in ethanol (30 mL). The reaction mixture was heated at reflux for 24 h then the mixture was cooled to room temperature. After 48 h, the precipitated yellow crystals were separated by filtration, washed with ethanol, and dried at $80\text{ }^{\circ}\text{C}$ for 12 h to give the salen ligand.

2.4 General Procedure for the Preparation of KCC-1/3-Bromopropyl NPs

Under nitrogen atmosphere, 2 mL of 3-Bromopropyltrimethoxysilane is added to 5.0 g of KCC-1 in suspension with 50 mL of freshly distilled toluene. After 24 h of reaction under reflux, the solid is filtered, washed thoroughly with toluene, ethanol, toluene, diethylether and then subjected to toluene Soxhlet extraction. The functionalized KCC-1 is finally dried in vacuum at $70\text{ }^{\circ}\text{C}$.

2.5 General Procedure for the Preparation of KCC-1/Salen NPs

The salen ligand (0.41 g) was dissolved in toluene (5 mL) and methanol (5 mL), respectively. The two solutions were combined and the reaction mixture was vigorously stirred at $60\text{ }^{\circ}\text{C}$ for 24 h then KCC-1/3-bromopropyl (0.6 g) was added. After stirring at $60\text{ }^{\circ}\text{C}$ for 24 h, the brown solid was separated by filtration, washed with ethanol, and dried under vacuum at $60\text{ }^{\circ}\text{C}$ for 24 h to afford KCC-1/Salen.

2.6 General Procedure for the Preparation of KCC-1/Salen/Ru(II) NPs

A mixture of KCC-1/Salen (0.45 g), $\text{Ru}(\text{DMSO})_4\text{Cl}_2$ (0.5 g), and Et_3N (0.8 mL) in methanol (10 mL) was degassed with N_2 and refluxed for 4 h. After cooling to room temperature, the precipitate was filtered and washed with methanol ($10\text{ mL} \times 3$) and ether ($10\text{ mL} \times 3$) to get a reddish-brown powder. The powder was mixed with an excess of 4-methylpyridine in methanol (0.5 mL) and heated to reflux for 2 h. The final particle was separated from the solution by applying a magnetic field, washed three times with water to remove any ions present, and dried under vacuum [42].

2.7 General Procedures for Preparation of 2-oxazolidinones

In a 100 mL stainless-steel reactor, CO_2 (1.0 MPa), propargylic amine (10 mmol), and KCC-1/Salen/Ru(II) (1 mg) were added at room temperature. Then, the temperature was raised to $100\text{ }^{\circ}\text{C}$ with the addition of CO_2 from a reservoir tank to maintain a constant pressure (2.0 MPa). The remaining CO_2 was removed slowly. After reaction, the catalyst was separated by filtration under vacuum and reused for further recycling experiment. The crude product mixture was dried over anhydrous sodium sulphate, and then subjected to column chromatography using a 6:1 petroleum ether/EtOAc eluent system on silica gel to give 2-oxazolidinones as a colorless liquid.

2.8 Spectral Data of Synthesized Compounds

3-butyl-5-methyleneoxazolidin-2-one (Compound 2a): Yellow oil; ^1H NMR δ = 0.90 (t, J = 7.2 Hz, 3H), 1.31–1.22 (m, 2H), 1.50–1.44 (m, 2H), 3.20 (t, J = 7.2 Hz, 2H), 4.14 (d, J = 2.4 Hz, 2H), 4.22 (d, J = 2.4 Hz, 2H), 4.64 (d, J = 2.4 Hz, 1H) ppm. ^{13}C NMR δ = 13.6, 19.5, 28.9, 43.5, 47.4, 85.9, 150.0, 155.2 ppm. GC-MS m/z (%) = 155 (90), 113 (27), 112 (100), 98 (11), 84 (37).

3-Methyl-5-methylene-1,3-oxazolidin-2-one (Compound 2b): Yellow oil; ^1H NMR δ = 2.89 (s, 3H), 4.14 (dd, J = 2.4 Hz, 2H), 4.30 (dt, J = 3.1 Hz, 1H), 4.72 (dt, J = 3.1 Hz, 1H) ppm. ^{13}C NMR δ = 30.4, 50.8, 86.5, 149.0, 156.1 ppm.

3-Methyl-5-ethylidene-1,3-oxazolidin-2-one (Compound 2c): White powder; mp 74–76 °C. ^1H NMR δ =1.64 (dt, J =7.0 Hz, 3H), 2.89 (s, 3H), 4.10 (dq, J =2.2 Hz, 2H), 4.60 (qt, J =7.0 Hz, 1H) ppm. ^{13}C NMR δ =9.6, 30.3, 50.0, 97.3, 141.3, 156.0 ppm.

3-Benzyl-5-ethylidene-1,3-oxazolidin-2-one (Compound 2d): White powder; mp 40–42 °C. ^1H NMR δ =1.65 (dt, J =7.0 Hz, 3H), 3.92 (dq, J =2.2 Hz, 2H), 4.42 (s, 2H), 4.53 (qt, J =7.0 Hz, 1H), 7.24–7.40 (m, 5H, Ar) ppm. ^{13}C NMR δ =9.9, 47.4, 47.9, 97.9, 128.0, 128.8, 135.2, 141.6, 156.3 ppm.

3-Isopropyl-5-ethylidene-1,3-oxazolidin-2-one (Compound 2e): Yellow oil; ^1H NMR δ =1.15 (d, J =6.5 Hz, 6H), 1.69 (dt, J =6.9 Hz, 3H), 4.02 (dq, J =2.2 Hz, 2H), 4.12 (septet, J =6.7 Hz, 1H), 4.60 (qt, J =7.0 Hz, 1H) ppm. ^{13}C NMR δ =9.9, 19.7, 42.9, 44.8, 97.3, 142.1, 155.3 ppm.

3-Methyl-5-benzylidene-1,3-oxazolidin-2-one (Compound 2f): White powder; mp 139–141 °C. ^1H NMR δ =2.94 (s, 3H), 4.30 (d, J =2.1 Hz, 2H), 5.49 (t, J =2.1 Hz, 1H), 7.19 (t, J =7.3 Hz, 1H), 7.30 (dd, J =7.3 Hz, J =7.6 Hz, 2H), 7.54 (d, J =7.6 Hz, 1H) ppm. ^{13}C NMR δ =30.5, 50.9, 102.9, 127.0, 128.2, 128.7, 133.5, 141.7, 155.6 ppm.

5-(4'-Methylbenzylidene)-3-methyl-1,3-oxazolidin-2-one (Compound 2g): White powder; mp 134–136 °C. ^1H NMR δ =7.47 (d, J =8.1 Hz, 2H), 7.15 (d, J =8.0 Hz, 2H), 5.50 (t, J =2.0 Hz, 1H), 4.30 (d, J =2.0 Hz, 2H), 3.00 (s, 3H), 2.31 (s, 3H). ^{13}C NMR δ =155.6, 140.6, 136.3, 130.5, 129.0, 127.9, 102.9, 50.8, 30.2, 21.0 ppm.

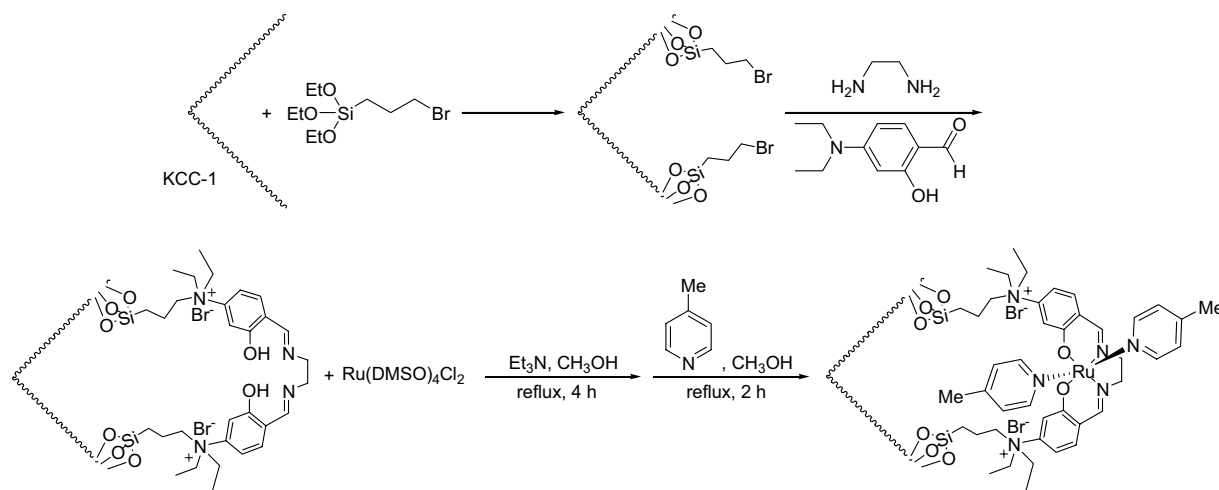
5-benzylidene-3-butyl-4-ethyloxazolidin-2-one (Compound 2h): Yellow oil; ^1H NMR δ =1.09 (m, 6H), 1.31–1.40 (m, 2H), 1.52–1.59 (m, 2H), 1.73–1.75 (m, 1H), 1.97–2.01 (m, 1H), 3.01–3.06 (m, 1H), 3.54–3.65 (m, 1H), 4.54 (s, 1H), 5.50 (s, 1H), 7.20 (dd, J =6.8 Hz, J =12.8 Hz, 1H), 7.34 (dd, J =7.2 Hz, J =12.8 Hz, 2H), 7.61 (d, J =7.6 Hz, 2H) ppm. ^{13}C NMR δ =6.3, 13.5, 20.1, 25.0, 29.1, 41.0,

58.9, 102.2, 126.5, 128.1, 133.8, 146.6, 155.3 ppm. GC-MS m/z (%)=259 (14), 230 (100), 174 (51), 118 (26), 90 (22).

3 Results and Discussion

The Salen-Ru Schiff base was covalently attached onto the surface of KCC-1 by a nucleophilic reaction, which resulted in dual catalytically active centers with a synergistic effect to greatly enhance the catalytic productivity. Furthermore, the catalyst can be easily recovered from the reaction mixture by centrifugation for steady reuse (Scheme 2).

The morphology and structure of the KCC-1 and KCC-1/Salen/Ru(II) NPs are further characterized by SEM. Figure 1a shows an SEM image of highly textured KCC-1 samples, where the samples have spheres of uniform size with diameters of ~300 nm and a wrinkled radial structure. A close inspection of these images shows that wrinkled fibers (with thicknesses of ~8.5 nm) grow out from the center of the spheres and are arranged radially in three dimensions. Also, the overlapping of the wrinkled radial structure forms cone-shaped open pores. The SEM image shows that the entire sphere is solid and composed of fibers. Furthermore, this open hierarchical channel structure and fibers are more easily for the mass transfer of reactants and increase the accessibility of active sites. The SEM images of KCC-1/Salen/Ru(II) NPs showed that after modification the morphology of KCC-1 is not change (Fig. 1b). After being reused ten times, the dandelion-like structure of the catalyst could be still observed although the dandelion-like structure collapsed to some extent. The structure similar between fresh KCC-1/Salen/Ru NPs and the KCC-1/Salen/Ru(II) NPs reused ten times, accounted for high power in recyclability (Fig. 1c).



Scheme 2 Schematic illustration of the synthesis for KCC-1/Salen/Ru(II) NPs

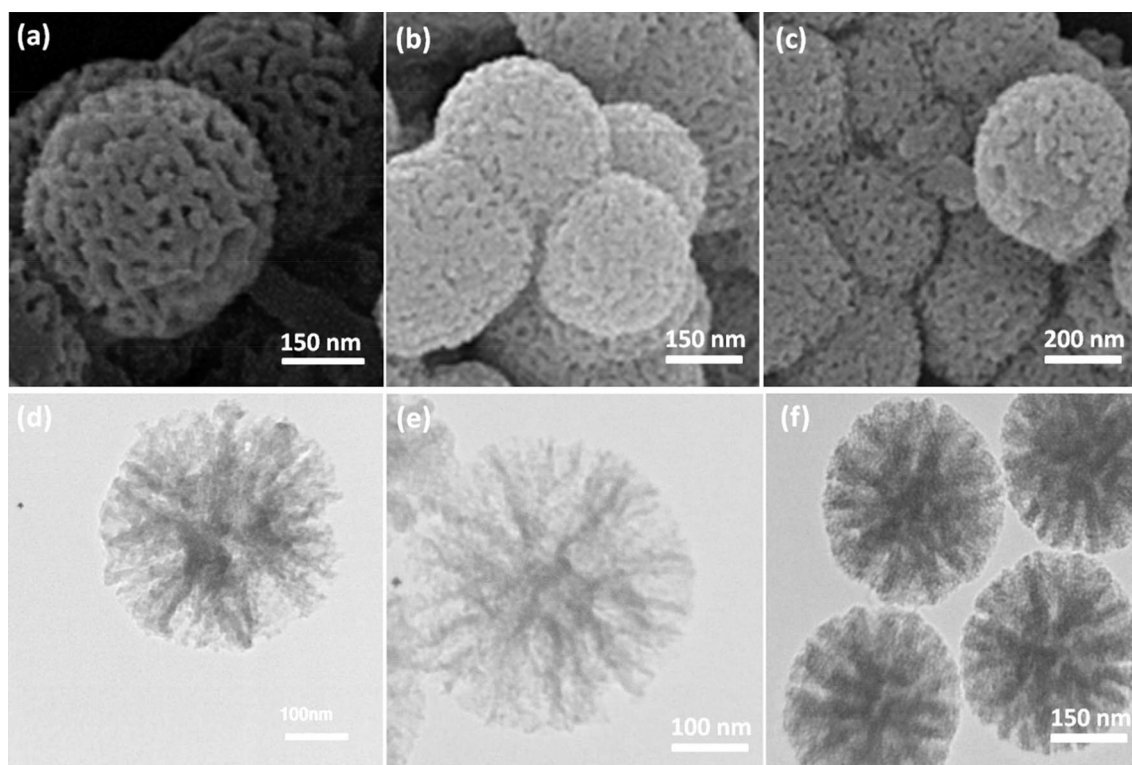


Fig. 1 SEM images of KCC-1 NPs (a); fresh KCC-1/Salen/Ru(II) NPs (b); KCC-1/Salen/Ru(II) NPs after ten reuses (c); TEM images of KCC-1 NPs (d); fresh KCC-1/Salen/Ru(II) NPs (e); KCC-1/Salen/Ru(II) NPs after ten reuses (f)

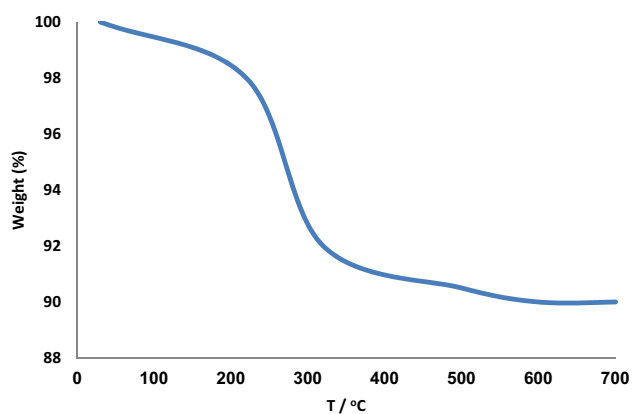


Fig. 2 TGA diagram of KCC-1/Salen/Ru(II) NPs

The thermal stability of the synthesized KCC-1/Salen/Ru(II) NPs catalyst was detected through TGA and the results are depicted in Fig. 2. The weight loss below 250 °C was ascribed to the elimination of the physisorbed and chemisorbed solvent on the surface of the silica material. About 8.2% of the weight loss, in the temperature range 250–450 °C, was due to the organic group derivatives.

The N_2 adsorption–desorption isotherms of KCC-1/Salen/Ru(II) NPs showed characteristic type IV curve

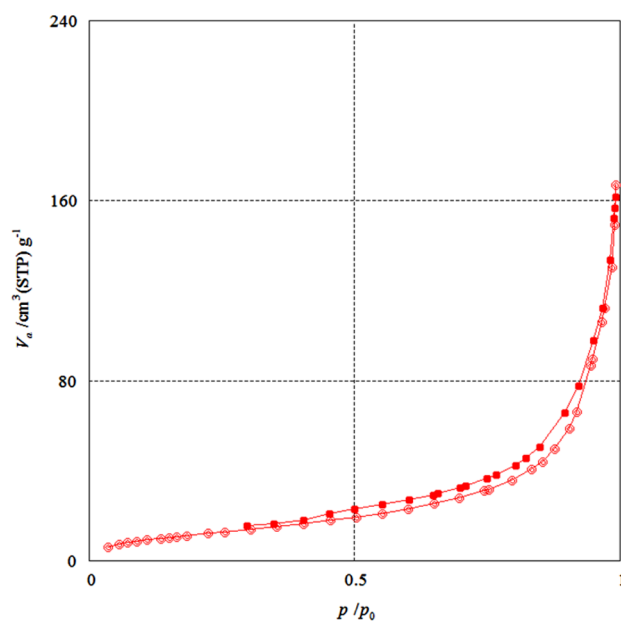


Fig. 3 Adsorption–desorption isotherms of KCC-1/Salen/Ru(II) NPs

(Fig. 3), which is consistent with literature reports on standard fibrous silica spheres. As for KCC-1, the BET surface area, total pore volume, and BJH pore diameter are obtained

as 439 m²/g, 1.49 cm³/g, and 14.78 nm respectively, whereas the corresponding parameters of KCC-1/Salen/Ru(II) NPs have decreased to 328 m²/g, 1.22 cm³/g, and 13.49 nm. The nitrogen sorption analysis of KCC-1/Salen/Ru NPs also confirms a regular and uniform mesostructure with a decrease in surface area, pore diameter and pore volume parameters in comparison with that of pristine KCC-1. With the functionalization by Salen/Ru-Si, the corresponding pore volumes are drastically reduced. This could be ascribed to increased loading with the sensing probe, which occupies a large volume inside the silica spheres (Fig. 3; Table 1).

FT-IR spectroscopy was employed to determine the surface modification of the synthesized catalyst (Fig. 4). The Si–O–Si symmetric and asymmetric stretching vibrations

at 802 and 1103 cm^{−1} and the O–H stretching vibration at 3444 cm^{−1} were observed for the KCC-1 (Fig. 4a). The bands observed at 3121 and 2929 cm^{−1} are assigned to C–H stretching of aromatic and aliphatic moieties. Moreover, the signals cleared at 1463 and 1535 cm^{−1} are, respectively, attributed to C=C and C=N. (Fig. 4b). These results indicated that the salen had been successfully introduced onto the surface of KCC-1.

To optimize the reaction conditions, the carbon dioxide and propargylic amine were used for the synthesis 2-oxazolidinone in the presence of KCC-1/Salen/Ru(II) NPs as a catalyst was chosen as a model system. The effect of various parameters such as solvent, and time (Table 2) were examined on the model reaction. To investigate the effect of solvents for the synthesis 2-oxazolidinone, different solvents have been used (Table 2, Entries 1–15) and the obtained results reveal that when the polar protic solvents, such as methanol, isopropanol, ethanol, and water are used, the expected product is not formed. However, the yield of the crosscoupling product was relatively average in polar aprotic solvents, such as DMF, EtOAc, and DMSO. When the reaction was conducted in less polar solvents, such as

Table 1 Structural parameters of KCC-1 and KCC-1/Salen/Ru(II) NPs materials determined from nitrogen sorption experiments

Catalysts	S_{BET} (m ² g ^{−1})	V_a (cm ³ g ^{−1})	D_{BJH} (nm)
KCC-1	439	1.49	14.78
KCC-1/Salen/ Ru NPs	328	1.22	13.49

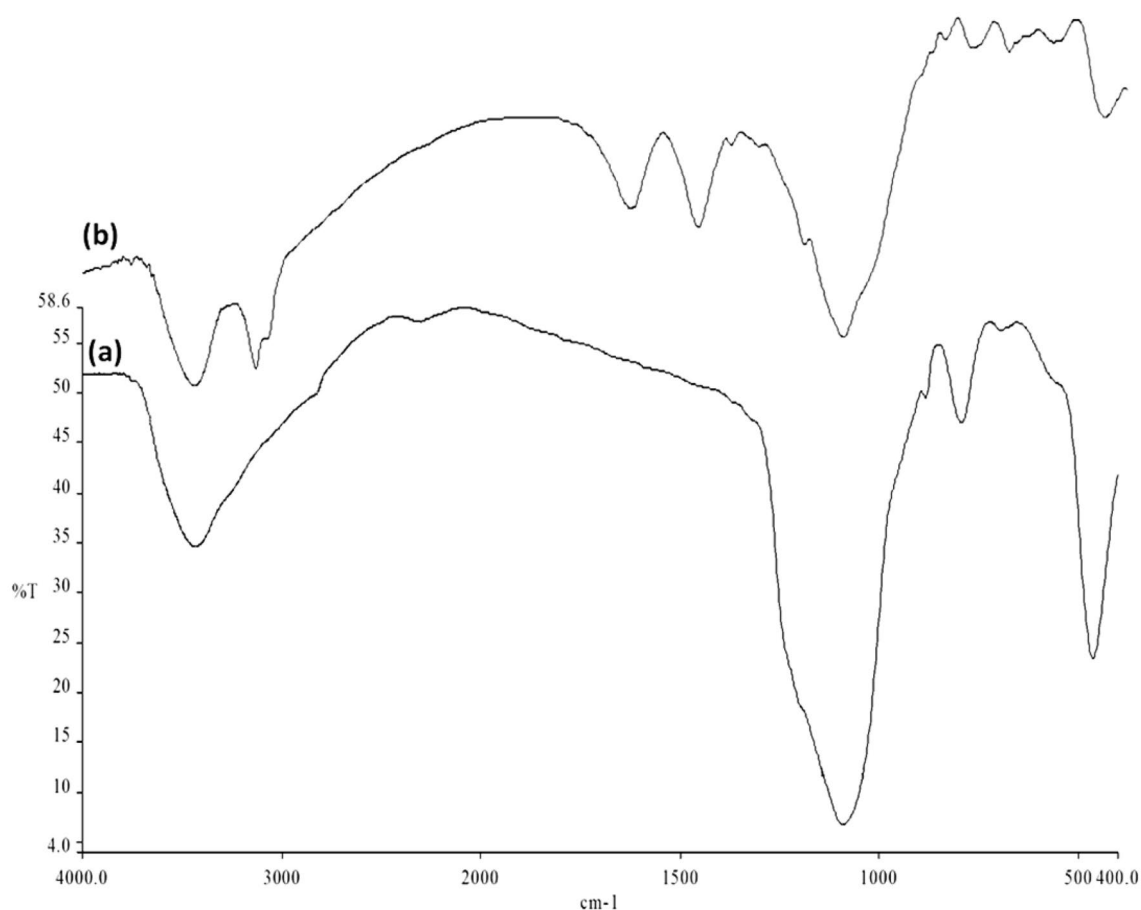


Fig. 4 FTIR spectra of **a** KCC-1 NPs, **b** KCC-1/Salen/Ru(II) NPs

Table 2 Synthesis of 2-oxazolidinone by KCC-1/Salen/Ru(II) NPs in different solvents

Entry	Solvent	Time (min)	Yield (%) ^a
1	EtOH	90	—
2	H ₂ O	90	—
3	CH ₃ CN	90	47
4	DMF	90	32
5	CH ₂ Cl ₂	90	35
6	EtOAc	90	46
7	THF	90	36
8	Toluene	90	50
9	<i>n</i> -Hexane	90	—
10	CHCl ₃	90	35
11	DMSO	90	40
12	MeOH	90	—
13	Dioxane	90	—
14	<i>i</i> -PrOH	90	—
15	Anisole	90	59
16	Solvent-free	90	97
17	Solvent-free	60	97
18	Solvent-free	30	89
19	Solvent-free	20	54
20	Solvent-free	10	21

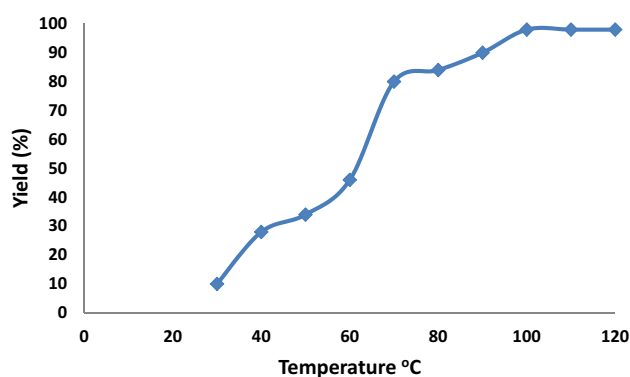
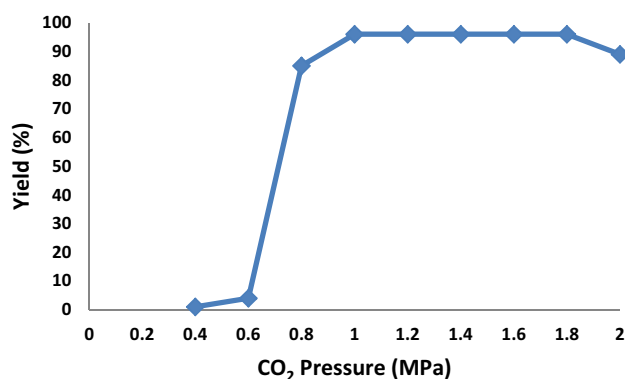
Reaction conditions: CO₂ (1.0 MPa), propargylic amine (10 mmol), KCC-1/Salen/Ru(II) NPs (1 mg), solvent (10 mL), at reflux or 100 °C

^aIsolated yields

anisole or toluene, average yields were isolated. However, the carbonylative cross-coupling product was obtained in low yield in polar solvents. In this study, it was found that conventional heating under solvent free is more efficient than using solvents (Table 2, Entries 16). Under the optimal conditions, the reaction progress for the shortest time necessary in the presence of 1 mg of KCC-1/Salen/Ru(II) NPs was monitored by GC, that excellent yields of synthesis of 2-oxazolidinone can be achieved in 60 min (Table 2, Entries 17).

To optimize reaction conditions for the KCC-1/Salen/Ru(II) NPs catalyst system, the effects of various reaction parameters were investigated. The influence of temperature on this reaction is exhibited in Fig. 5. It is obvious that the 2-oxazolidinone yield increased up to 97% at 100 °C under 2.0 MPa CO₂ pressure over 60 min. Whereas further increase in the temperature resulted in a slight decrease in the product yield due to formation of a small amount of by-products. Therefore, the optimal temperature for the coupling reaction of CO₂, and propargylic amine are 100 °C.

As shown in Fig. 6, the CO₂ pressure also has a significant effect on the coupling reaction. The reaction rate was accelerated quickly in the range 0.8–1.0 MPa. However, the yield decreased when the pressure reached 2.0 MPa. Based on these report, it can be inferred that increasing reaction

**Fig. 5** Effect of temperature on yield of 2-oxazolidinone**Fig. 6** Effect of CO₂ pressure on the synthesis of 2-oxazolidinone

pressure was propitious to produce 2-oxazolidinone when the reaction pressure was less than 1.8 MPa. Too high pressures would reduce the propargylic amine concentration to give low 2-oxazolidinone yields. Therefore, the CO₂ pressure of 1.0 MPa was considered as suitable condition.

For further investigation the efficiency of the catalyst, different control experiments were performed and the obtained information is shown in Table 3. Initially, a

Table 3 Influence of different catalysts for synthesis of 2-oxazolidinone

Entry	Catalyst	Yield (%) ^a
1	KCC-1	—
2	KCC-1/Salen	—
3	KCC-1/Salen/Ru(II)	97
4	Nano-SiO ₂ /Salen/Ru(II)	49
5	MCM-41/Salen/Ru(II)	81
6	SBA-15/Salen/Ru(II)	86
7	Salen/Ru(II)	98

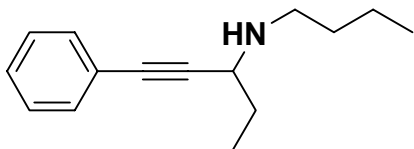
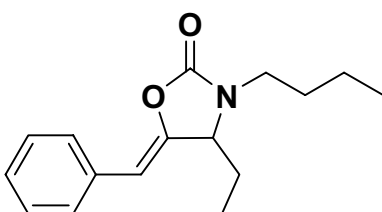
Reaction conditions: CO₂ (1.0 MPa), propargylic amine (10 mmol), KCC-1/Salen/Ru(II) NPs (1 mg) at 100 °C

^aIsolated yield

Table 4 Synthesis of 2-oxazolidinone derivatives catalyzed by KCC-1/Salen/Ru(II) NPs

Entry	Amines	2-oxazolidinones	Products	Yield (%) ^a
1			2a	94
2			2b	97
3			2c	93
4			2d	92
5			2e	98
6			2f	95
7			2 g	96

Table 4 (continued)

Entry	Amines	2-oxazolidinones	Products	Yield (%) ^a
8			2f	93

Reaction condition: propargylic amine derivatives (1 mmol), and CO₂ 1 MPa, KCC-1/Salen/Ru(II) NPs (1 mg), 60 min and at 100 °C

^aYield refers to isolated product

standard reaction was carried out using KCC-1 showed that any amount of the desired product was not formed after 60 min of reaction time (Table 3, entries 1). Also, when KCC-1/Salen was used as the catalyst, a reaction was not observed (Table 3, entries 2). The Salen could not give the satisfactory catalytic activity under mild reactions. Based on these disappointing results, we continued the studies to improve the yield of the product by added the Ru(II). Notably, there was not much difference in the reaction yields when reaction was carried out using KCC-1/Salen/Ru(II) NPs and Salen/Ru(II) catalyst (Table 3, entries 3 and 7). However, Salen/Ru(II) is not recoverable and reusable for the next runs. These observations show that the reaction cycle is mainly catalyzed by Ru(II) species complexed on the KCC-1/Salen nanostructure. The nano-sized particles increase the exposed surface area of the active site of the catalyst, thereby enhancing the contact between reactants and catalyst dramatically and mimicking the homogeneous catalysts. As a result, KCC-1/Salen/Ru(II) NPs was used in the subsequent investigations because of its high reactivity, high selectivity and easy separation. Also, the activity and selectivity of nano-catalyst can be manipulated by tailoring chemical and physical properties like size, shape, composition and morphology. To assess the exact impact of the presence of KCC-1 in the catalyst, the KCC-1/Salen/Ru(II) NPs compared with MCM-41/Salen/Ru(II), SBA-15/Salen/Ru(II), and nano-SiO₂/Salen/Ru(II). When nano-SiO₂/Salen/Ru(II), MCM-41/Salen/Ru(II) or SBA-15/Salen/Ru(II) was used as the catalyst, the yield of the desired product was average to good, but the yield for KCC-1/Salen/Ru(II) NPs was excellent. Non-negligible activity of the silica was attributed to its shape, composition and morphology. Besides, the large space between fibers can significantly increase the accessibility of the active sites of the KCC-1. That is why, the KCC-1 was more effective than nano-SiO₂, MCM-41, and SBA-15 (Table 3, entries 3–6). As a result, KCC-1 NPs were used in the subsequent investigations because of its high reactivity, high selectivity and easy separation (Table 3).

The carboxylative cyclization for a variety of propargylic amines was then under taken to explore the scope of this well developed KCC-1/Salen/Ru(II) NPs catalytic system. As shown in Table 4, both aromatic and aliphatic propargylic amines performed smoothly to give the corresponding 2-oxazolidinones in excellent yields.

For further investigation the possibility of the heterogeneous nature of KCC-1/Salen/Ru(II) NPs, a kinetic study was performed. For this purpose, ruthenium leaching was study for synthesis of 2-oxazolidinone under the optimized reaction condition. To determine the Ru(II) concentration in solution, six samples of the reaction mixture were taken during the reaction. The samples were analyzed by ICP-MS as well as the yield of the reaction was monitored by GC. The results were described in Fig. 7. No obvious leaching was observed, according to the ICP-MS data. According to the obtained results, the conclusion could be derived that the heterogeneous ruthenium species aren't the catalyst promoter in this reaction.

To gain insight into the nature of the nanocatalyst, a three-phase test was designed. Three-phase test is a powerful technique that allows the catalyst to be in its nature habitat. To conduct the test, the model synthesis of 2-oxazolidinone was carried out in the absence and in the presence of salen as a strong scavenger to capture the homogeneous soluble ruthenium ions. The reaction progress was monitored by GC. As it is evident in Fig. 8, the presence of scavenger has no effect on the yield of the reaction. All of the results obtained from heterogeneity tests confirmed that the KCC-1/Salen/Ru(II) NPs had a high catalytic activity with a truly stable heterogeneous nature under the described reaction conditions.

It is important to note that the heterogeneous property of KCC-1/Salen/Ru(II) NPs facilitates its efficient recovery from the reaction mixture during work-up procedure. The activity of the recycled catalyst was also examined under the optimized conditions. After the completion of reaction, the catalyst was separated by

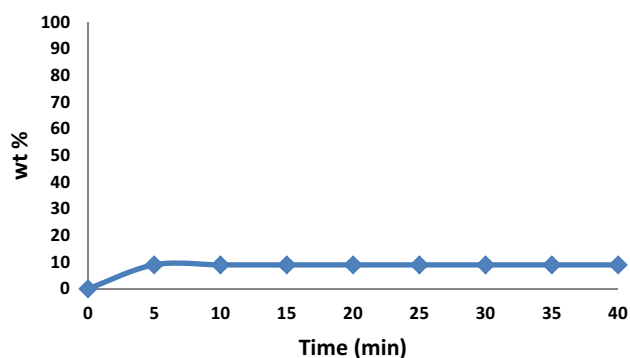


Fig. 7 Time-dependent correlation of the ruthenium leaching in model reaction

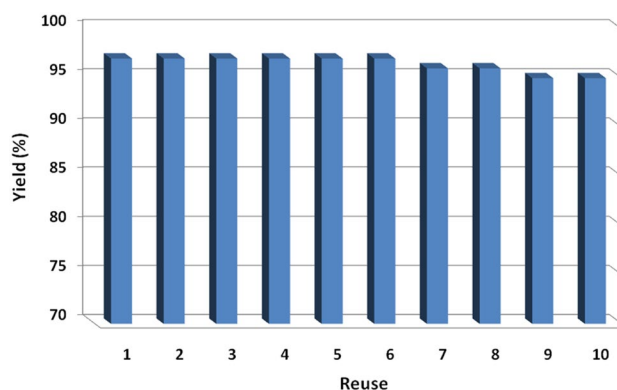


Fig. 9 The reusability of catalysts for synthesis of 2-oxazolidinone

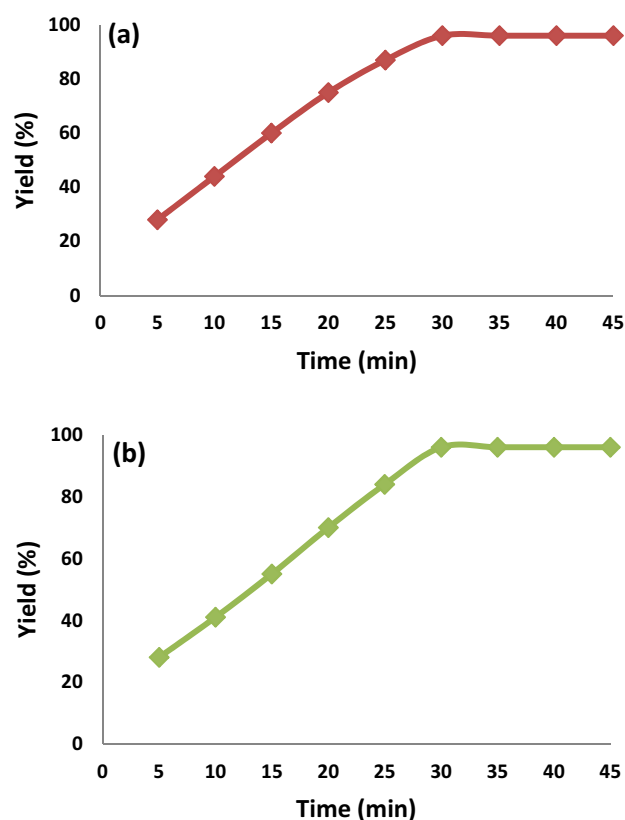


Fig. 8 Time-dependent correlation of the yield of 2-oxazolidinone in the absence (a) and in the presence (b) of salen

filtration, washed with methanol and dried at the pump. The recovered catalyst was reused for ten consecutive cycles without any significant loss in catalytic activity (Fig. 9). This lack of reduction in catalyst performance can be attributed to the simple and stability of the catalyst structure.

4 Conclusions

In the present study KCC-1/Salen/Ru(II) NPs was synthesized and characterized as an environmentally-friendly nanocatalyst for the synthesis of 2-oxazolidinones with various electronically diverse substrates. The experimental results displayed the core-shell structure of the synthesized catalyst with a mean size range of 250–300 nm. In addition, the catalyst was easily recoverable and reusable. Subsequently, high yields in short reaction times were achieved without the need for an expensive catalyst as well as excellent reusability for at least ten times in the corresponding reaction without a reduction in catalytic activity.

Acknowledgements The authors gratefully acknowledge the financial support of Islamic Azad University, Bojnourd Branch, Bojnourd, Iran.

References

- Polshettiwar V, Cha D, Zhang X, Basset JM (2010) *Angew Chem Int Ed* 49:9652–9656
- Maity A, Polshettiwar V (2017) *ChemSusChem* 10:3866–3913
- Kundu PK, Dhiman M, Modak A, Chowdhury A, Polshettiwar V (2016) *ChemPlusChem* 81:1142–1146
- Gautam P, Dhiman M, Polshettiwar V, Bhanage BM (2016) *Green Chem* 18:5890–5899
- Fihri A, Cha D, Bouhrara M, Almana N, Polshettiwar V (2012) *ChemSusChem* 5:85–89
- Sadeghzadeh SM (2016) *J Mol Catal A* 423:216–223
- Sadeghzadeh SM (2016) *Catal Sci Technol* 6:1435–1441
- Sadeghzadeh SM (2015) *Catal Commun* 72:91–96
- Sadeghzadeh SM (2015) *Green Chem* 17:3059–3066
- Dong Z, Le X, Li X, Zhang W, Dong C, Ma J (2014) *Appl Catal B* 158–159:129–135
- Pinaka A, Vougioukalakis GC (2015) *Coord Chem Rev* 288:69–97
- Olajire AA (2013) *J CO₂ Util* 3–4:74–92
- Mikkelsen M, Jorgensen M, Krebs FC (2010) *Energy Environ Sci* 3:43–81
- Kuwahara Y, Yamashita H (2013) *J CO₂ Util* 1:50–59
- Omae I (2012) *Coord Chem Rev* 256:1384–1405

16. Razali NAM, Lee KT, Bhatia S (2012) *Renew Sustain Energy Rev* 16:4951–4964
17. Lu XB, Ren WM, Wu GP (2012) *Acc Chem Res* 45:1721–1735
18. Yu B, Diao ZF, Guo CX, He LN (2013) *J CO₂ Util* 1:60–68
19. Pulla S, Felton CM, Ramidi P, Gartia Y, Ali N, Nasini UB, Ghosh A (2013) *J CO₂ Util* 1:49–57
20. Aresta M, Dibenedetto A, Angelini A (2013) *J CO₂ Util* 3–4:65–73
21. Lang XD, Liu XF, He LN (2015) *Curr Org Chem* 19:681–694
22. Sattar A, Esmail V, Marjan S, Akram H, Ahmedreza B (2017) *J CO₂ Util* 19:120
23. Pulla S, Felton CM, Ramidi P (2013) *J CO₂ Util*, 2:49–57
24. Maggi R, Bertolotti C, Orlandini E, Oro C, Sartori G, Selva M (2007) *Tetrahedron Lett* 48:2131–2134
25. Kayaki Y, Yamamoto M, Suzuki T, Ikariya T (2006) *Green Chem* 8:1019–1021
26. Feroci M, Orsini M, Sotgiu G, Rossi L, Inesi A (2005) *J Org Chem* 70:7795–7798
27. Mitsudo T, Hori Y, Yamakawa Y, Watanabe Y (1987) *Tetrahedron Lett* 28:4417–4418
28. Shi M, Shen Y-M (2002) *J Org Chem* 67:16–21
29. Yoshida M, Mizuguchi T, Shishido K (2012) *Chem Eur J* 18:15578–15581
30. Yuan R, Lin Z (2015) *ACS Catal* 5:2866–2872
31. Crutchky RJ (1994) *Adv Inorg Chem* 41:273
32. Nag S, Gupta P, Butcher RJ, Bhattacharya S (2004) *Inorg Chem* 43:4814–4816
33. Acharyya R, Peng S-M, Lee GH, Bhattacharya S (2003) *Inorg Chem* 42:7378
34. Koiwa T, Masuda Y, Shono J, Kawmoto Y, Hashino Y, Hashimoto T, Natarajan K, Shimizu K (2004) *Inorg Chem* 43:6215–6223
35. Novakova O, Kasparkova J, Vrana O, Vanvliet PM, Reedijk J, Brabec V (1995) *Biochemistry* 34:12369–12378
36. Frey GD, Bell ZR, Jeffery JC, Ward MD (2001) *Polyhedron* 20:3231–3237
37. Vigato PA, Tamburini S (2004) *Coord Chem Rev* 248:1717–2128
38. Miller JA, Gross BA, Zhuravel MA, Jin W, Nguyen ST (2005) *Angew Chem* 117:3953–3957
39. Man WL, Kwong HK, Lam WWY, Xiang J, Wong TW, Lam WH, Wong WT, Peng SM, Lau TC (2008) *Inorg Chem* 47:5936–5944
40. Che CM, Poon CK (1998) *Pure Appl Chem* 60:1201–1207
41. Che CM, Tang WT, Wong WT, Lai TF (1989) *J Am Chem Soc* 111:9048
42. Leung WH, Chan EYY, Chow EKF, Williams ID, Peng SM (1996) *J Chem Soc Dalton Trans* 7:1229
43. Bhunia S, Molla RA, Kumari V, Islam SM, Bhaumik A (2015) *Chem Commun* 51:15732–15735
44. Noh EK, Na SJ, Kim W, Lee SSS BY (2007) *J Am Chem Soc* 129:8082–8083
45. An Q, Li Z, Graff R, Guo J, Gao H, Wang C (2015) *ACS Appl Mater Interfaces* 7:4969–4978
46. Tian D, Liu B, Gan Q, Li H, Darensbourg DJ (2012) *ACS Catal* 2:2029–2035
47. Darensbourg DJ, Chung WC, Wilson SJ (2013) *ACS Catal* 3:3050–3057
48. Li Z, Wu S, Ding H, Zheng D, Hu J, Wang X, Huo Q, Guan J, Kan Q (2013) *New J Chem* 37:1561–1568
49. Jiang Y, Li F, Huang F, Zhang B, Sun L (2013) *Chin J Catal* 34:1489–1495